RSC Advances

ROYAL SOCIETY OF CHEMISTRY

www.rsc.org/advances

Journal Name

ARTICLE

Remarkable Efficacy of Graft Block Copolymers as Surfactants in Reducing Interfacial Tension

Received 00th January 20xx,
Accepted 00th January 20xx

DOI: 10.1039/x0xx00000x

www.rsc.org/

Yang Zhou,*[a,§] Chun Zhou,[a,b,§] Xinping Long,[a] Xianggui Xue,[a] Wen Qian,[a] and Shikai Luo[a]

Graft copolymers as surfactants have the larruping ability in improving interfacial properties of polymer blends or fluid mixtures. It is obviously related to the topologies of grafts. Based on dissipative particle dynamics (DPD) simulations, we investigated the interfacial properties (interfacial density, interfacial thickness and interfacial tension) of oil/water systems and their dependence on the topological structure and the concentration of graft copolymers. Importantly, a quantitative scaling relation between the variation of interfacial tensions $\Delta\gamma_S$ and the concentration C_S is firstly established as $\Delta\gamma_S=kC_S^N$. The exponent N is mainly dominated by graft numbers, for example, N=1.54 for $A_8(B_8)_1$ (1 graft) < N=1.63 for $A_8(B_4)_2$ (2 grafts) < N=1.73 for $A_8(B_2)_4$ (4 grafts). It means that graft copolymers with more grafts have the higher efficacy in reducing interfacial tensions at the same concentration. Further analysis by Gibbs adsorption isotherm is in accordance with the results of our simulated density profiles, which testify the credibleness of our established relation. This work provides a standard model for experimental applications of graft copolymers as surfactants, especially in reducing the interfacial tensions.

1. Introduction

In the past two decades, amphiphilic block copolymers as surfactants have attracted much attention, and have also broad applications in pharmaceutical, agrochemicals, dyestuffs, detergents, plastic, especially petroleum industries. Compared with typical small-molecule surfactants, the diversity in the molecular structure (such as linear, cyclic, star, multiblock, graft, etc.) of polymeric surfactants allows for extensive variation in their solution and interfacial properties and their practical applications.[1] Therefore, it is crucial to discover the link between the molecular structure of the surfactant and its physicochemical behaviour, although the correlative studies have had a long history. Among many properties, the interfacial tension (IFT) is a key essence. For small-molecule surfactants, there has been several profound understanding. The earlier Traube's rule showed that increasing the hydrophobic tail length makes them more efficient in reducing the interfacial tension.[2] Rekvig et al found that branched surfactants are more efficient than linear ones only if the head repulsion is sufficiently strong.[3] Furthermore, the simulation technique as an effective means are often used to explain the molecular mechanism of small-molecular surfactants at the interface.[4] As for amphiphilic polymeric surfactants, graft (branch or brush) copolymers (GCPs) have made great progress in recent years, especially in the biomedical field.[1] Lodge and co-workers used polyethylene-*graft*-poly(methyl methacrylate) (PE-*g*-PMMA) as compatibilizers for binary PE/PMMA blends, and found that the graft copolymer with the shortest side chains was the most effective compatibilizer.[5] Kim and Jo used polythiophene-*graft*-poly(methyl methacrylate) as dispersants for poly(styrene-*co*-acrylonitrile)/ carbon nanotube composites, and yielded the enhanced mechanical properties.[6] John and co-workers used the mixture of hydrophobically grafted chitosans and common dispersants (Corexit 9500A) to enhance the stability of crude oil droplets in saline water.[7] Moreover, the polymer-grafted nanoparticles were also used as emulsifiers to prepare Pickering emulsions[8] and emulsion polymerizations.[9] Recently, it is more interesting that several novel shaped GCPs, such as double-brush copolymers,[10] ternary graft copolymers,[11] giant bottlebrush block copolymers,[12] are prepared and used as surfactants. In despite of many pioneer works, we still lack the molecular-level understanding of the relation between the topological structure and improving interfacial properties for polymeric surfactants, especially for the new GCPs. Actually, Eastwood and Dadmun investigated the effect of topologies for multiblock copolymers on compatibilizing the PS/PMMA blends.[13] Li et al studied the role of topological structure for linear-, cyclic-, multiblock amphiphilic polyelectrolytes on stabilizing the latex particle in emulsion polymerization.[14] The experiments have shown several qualitative knowledge of the notable influence of topologies on the ability of polymers as surfactants. Obviously, the quantitative understanding for GCP as surfactants is still being starved for the more investigations. However, this is a challenge for the experiment because of the difficulty of preparing a set of GCPs with an absolute identical

[a] Institute of Chemical Materials, Chinese Academy of Engineering and Physics, 621010 Mianyang, China. E-mail: zhouy@caep.cn.
[b] School of Materials Science and Engineering, Southwest University of Science and Technology, 621010 Mianyang, China.

chemical component but different topological structures. Computer simulations are a good choice to make up the lack of experiments.[4] At first, molecular dynamics (MD) methods have been widely applied to provide the detailed molecular-level information of surfactants at the interface.[15] However, MD is computationally too expensive to obtain the mesoscopic behaviour. Accordingly, the mesoscale dissipative particle dynamics (DPD) technique becomes a well-content tool. Groot and Warren emphatically mentioned the calculation of interfacial tensions when they pioneered the important relationship between DPD and Flory-Huggins theory.[16] Maiti and McGrother revisited the Groot-Warren theory and showed the computed interfacial tension of binary solvents in excellent agreement with experimental results.[17] Ginzberg et al also validated the reliability of DPD-based interfacial tensions by showing a good agreement among DPD, self-consistent field theory and experiments.[18] Li et al revealed the effect of the typical cetyltrimethylammonium bromide on the interfacial property of oil/water systems.[19] Striolo et al studied interfacial behaviours of homogeneous and Janus nanoparticles at the oil/water interface.[20] Qian et al investigated the interfaces in immiscible binary polymer blends and in the ternary systems with their block copolymers.[21] We also focused on the efficacy of special surfactants, such as small-molecular plasticizers, homogeneous nanorods, in improving interfacial properties of polymer blends.[22] Additionally, by self-consistent mean field methods and analytical theory, Balazs et al investigated the effect of the architectures of block copolymers (such as stars, combs) on the ability to reduce the interfacial tension for polymer blends.[23]

As for the significant oil/water system, the effect of GCPs as surfactants on their interfacial properties should not be ignored. Herein, we investigate the efficacy of GCP surfactants in improving the interfacial property using DPD simulations. We build a set of coarse-grained models of GCPs with the absolute identical component but different graft arranges, and elucidated how the topological structures affect their corresponding ability of decreasing the interfacial tension. The quantitative relationship between the interfacial tension and the graft degree was established and discussed in detail.

2. Method and Model Details

DPD, firstly developed by Hoogerbrug and Koelman,[24] is a coarse-grained particle-based simulation technique, which allows the larger length and longer time scale. DPD particles obey Newton's equation of motion, and the forces between pair non-bonded DPD particles include a conservative force $\boldsymbol{F}^{C}$, a dissipative force $\boldsymbol{F}^{D}$, and a random force $\boldsymbol{F}^{R}$, respectively. The bonded DPD particles are described by a harmonic spring force $\boldsymbol{F}^{S}$. Therefore, the total force is expressed by

$$f_i = \sum_{i \neq j} (F_{ij}^{C} + F_{ij}^{D} + F_{ij}^{R} + F_{(i,i+1)}^{S}) \quad (1)$$

The three forces for the non-bonded interaction are given by

$$\begin{aligned} F_{ij}^{C} &= -a_{ij} w^{C}(r_{ij}) \mathbf{e}_{ij} \\ F_{ij}^{D} &= -\gamma w^{D}(r_{ij})(\mathbf{e}_{ij} \cdot \mathbf{v}_{ij}) \mathbf{e}_{ij} \\ F_{ij}^{R} &= \sigma w^{R}(r_{ij}) \xi_{ij} \Delta t^{-0.5} \mathbf{e}_{ij} \end{aligned} \quad (2)$$

where $\mathbf{r}_{ij}=\mathbf{r}_i-\mathbf{r}_j$, $r_{ij}=|\mathbf{r}_{ij}|$, $\mathbf{e}_{ij}=\mathbf{r}_{ij}/r_{ij}$ and $\mathbf{v}_{ij}=\mathbf{v}_i-\mathbf{v}_j$. ζ_{ij}, a Gaussian random number with zero mean and unit variance. α_{ij}, the repulsion parameter between bead *i* and *j*, which reflects the chemical characteristics of interacting beads. γ, the friction constant and σ, the noise strength. For ensuring the system to satisfy the fluctuation-dissipation theorem and correspond to the Gibbs Canonical ensemble, only one of the two weight functions w^D and w^R can be chosen arbitrarily and this choice fixes the other one. There is also a relation between the amplitudes (σ and γ) and k_BT. It is $w^D=(w^R)^2$ and $\sigma^2=2\gamma k_BT$, k_B is the Boltzmann constant and T is the temperature.[25] Generally, the simple form for $w^C=w^D=(w^R)^2=(1-r_{ij})^2$ and $\sigma=3$ (*i.e.* $\gamma=4.5$) are chosen, and Newton equations for all beads are integrated by a modified version of the velocity-Verlet algorithm with $\lambda=0.65$.[16]

The spring force $\boldsymbol{F}^{S}$ for bonded beads is

$$F_{(i,i+1)}^{S} = -\sum_{i} k_S (l_{(i,i+1)} - l_0) \quad (3)$$

where $l_{(i,i+1)}$ is the bond length between connected two bead *i* and *i*+1. Here, the spring coefficient $k_S=4$ and the balance bond length $l_0=0$ are chosen. For easy numerical handling, the cutoff radius (r_c), the bead mass (m), and the temperature (k_BT) are chosen as the unit of the simulated system.

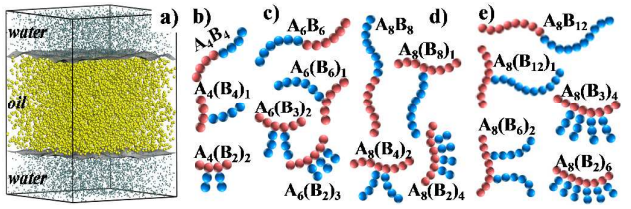

Fig. 1 a) The binary system containing water and oil yields two planar interfaces. Aqua and yellow beads represent water (W) and oil (O), respectively. b)-e), Models for four series of graft copolymer surfactants with different topologies, respectively. Pink and blue beads represent the hydrophilic chain (A) and the lipophilic grafts (B), respectively. b) for A4b4 series; c) for A6b6 series; d) for A8b8 series; e) for A8b12 series.

Figure 1 gives the typical setup of the oil/water mixture with two planar interfaces. Water and oil are described by a single bead. The simulation box size is $L_x \times L_y \times L_z = 30 \times 30 \times 40 r_c^3$, which contains 108000 beads ($\rho=3$). Periodic boundary conditions are implemented along the three directions. Here, we mainly focus on the interfacial properties, not dynamic process. Therefore, we build two interfaces within one simulation box by dividing three regions along the *z* direction, and then place water and oil beads, respectively, as shown in Figure 1a. The two interfaces are perpendicular to the *z* axis and always planar. The artificial initial configuration can speed up the formation of the interface, hence saving the computational cost. Figure 2 gives the coarse-grain models for 5 series of GCPs with the different topologies. For example, as shown in Figure 1b, A_4B_4

denotes a linear diblock copolymer composed of 4 beads of A and B block, respectively. $A_4(B_2)_2$ represents a graft copolymer, where A block with 4 beads is a main chain, two B blocks with 2 beads, respectively, are side chains. All three copolymers in Figure 1b are called as "A4B4 series". They would be randomly placed in the whole box, when exploring their effect on the interfacial properties. The time step Δt is 0.05 and a total of $2\sim6\times10^6$ DPD time steps are carried out to guarantee the equilibration for each system.

Table 1 Repulsion parameters (DPD unit) in this work

	W	O	A	B
W	25	100	25	100
O		25	100	25
A			25	100
B				25

Table 1 list the interaction parameters used in this work. Our main aim is to obtain the general rules of GCPs in reducing the interfacial tension. Therefore, we don't care the relationship between the chosen parameters and the real system. To obtain the sharp interfaces and bigger interfacial tensions, the repulsive parameter α_{WO}=100, which is also close to that used by Wang et al,[26] are chosen to describe the oil/water interfaces. Other parameters, $\alpha_{AW}=\alpha_{BO}$=25 and $\alpha_{AO}=\alpha_{BW}$=100, are used to represent the hydrophilicity of main chains (represented by bead A) and the lipophilicity of graft chains (B). All parameters are fixed except for the concentration of GCPs, it is to eliminate the influence of interactions, and focus on the influence of topologies more effectively.

3. Results and Discussions

The concentration (C_S) used in our simulation is represented by the volume fraction of GCPs (φ_{GCP}) in the ternary systems, *i.e.* $\varphi_{GCP}=N_{GCP}/(N_W+N_O+N_{GCP})$, where N_W and N_O are the number of W (water) and O (oil) beads, respectively. $N_{GCP}=N_A+N_B$ and N_A and N_B are the number of A and B beads in the system, respectively. The interfacial tension (γ_S) is calculated as

$$\gamma_S = \frac{1}{2}L_z\left\langle P_{zz} - \frac{P_{xx}+P_{yy}}{2}\right\rangle \quad (4)$$

where P_{ij} is the ij element of the pressure tensor, L_z is the simulation box length perpendicular to interface, and angular bracket denotes ensemble averages.[27]

For the different concentrations of φ_{GCP}=0.01, 0.05 and 0.09, Figure 2, 3 and 4 take the water/oil systems with A6B6 series of GCP surfactants as examples and give the adsorption processes of surfactants at the interface, equilibrium space structures and interfacial tensions, respectively. Based on the evolution of γ_S in Figure 2a, we can see that the pure water/oil system quickly arrive at the equilibrium point after about 2×10^5 steps. A steady average of the interface tension is calculated to 4.123±0.002 (DPD unit), which will be designated as γ_0 in the following context. In Figure 2b-2e, the small content of A_6B_6, $A_6(B_6)_1$, $A_6(B_3)_2$ and $A_6(B_2)_3$ are kept to be 0.01 and then added into the water/oil system, respectively. Based on the evolution of γ_S and the full adsorption of surfactants at the interface (inline image in Figure 2e), it can judge that 1×10^6 simulation steps are enough to arrive at the equilibrium for the ternary systems. Therefore, we adopt the average value of interfacial tensions in the latter 5×10^5 steps as the final results. Because the concentration of φ_{GCP}=0.01 is far from the critical micelle concentration (CMC) of the systems, the effect of GCPs as surfactants on the interfacial tension doesn't behave remarkably, for example, $\gamma_{S,A6(B3)2}$=4.059±0.003 (Figure 2d) is very close to $\gamma_{S,A6(B2)3}$=4.054±0.003 (Figure 2e).

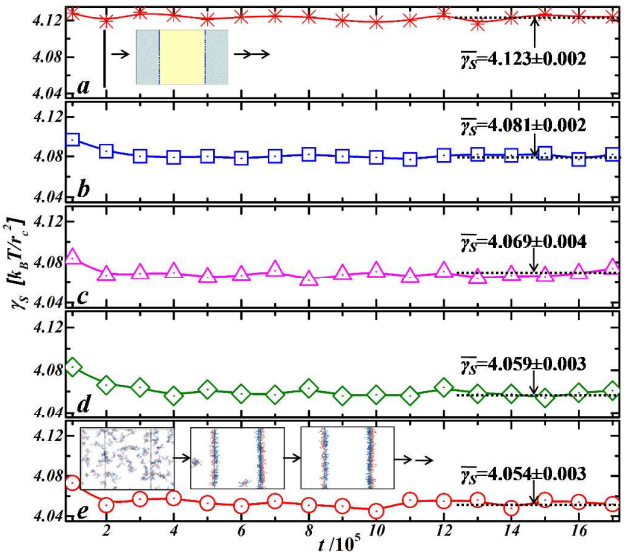

Fig. 2 The evolution of the interface tension γ_S with the simulation time t at φ_{GCP}=0.01. *a*) for the pure binary system of water/oil without the GCPs; *b*) for the ternary system of water/oil/A_6B_6; *c*) water/oil/$A_6(B_6)_1$; *d*) water/oil/$A_6(B_3)_2$; e) water/oil/$A_6(B_2)_3$.

Figure 3 and 4 give the adsorption conformation of GCPs at the interface and the evolution of γ_S with the simulation time t for φ_{GCP}=0.05 and 0.09, respectively. Comparing with the results at φ_{GCP}=0.01, the ternary system with higher concentrations need a longer simulation time, about more than 4×10^6 for φ_{GCP}=0.05 and more than 5×10^6 for φ_{GCP}=0.09, to reach the final equilibrium state. In fact, before the final equilibrium, the ternary systems can form the metastable conformations containing several micelles, such as those in Figure 3a1-d1 and in Figure 4a1-d1, which also have a steady γ_S value during a quite widen time range (see Figure 3a2-d2 and Figure 4a2-d2). It is easy to bring a mistake that φ_{GCP}=0.05 is the CMC for these polymeric surfactants. However, the GCPs forming the micelles can slowly sorb into the interface of water/oil by an additional simulation times (Figure 3a3-d3 and Figure 4a3-d3). Meanwhile, the final γ_S data in Figure 3a4-d4 and Figure 4a4-d4 observably decrease, comparing with those from metastable states. In addition, for φ_{GCP}=0.09, the ternary systems still have a few of micelles in the last equilibrium state, which testifies that the adsorption of GCPs at the interface arrives at the saturation. Here, we define φ_{GCP}=0.09 as the CMC of graft copolymers for our simulation systems. Considering the fact that the interfacial tension would not change significantly after CMC, therefore, we chose the

following concentrations of φ_{GCP}=0.01, 0.03, 0.05, 0.07 and 0.09, then the corresponding results represent the reality before the system achieves at the CMC level of surfactants.

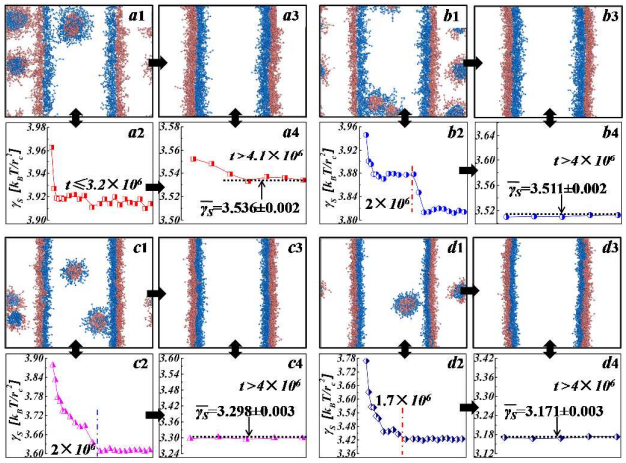

Fig. 3 The evolution of the interface tension γ_S with the simulation time t at φ_{GCP}=0.05. *a*) water/oil/A_6B_6; *b*) water/oil/$A_6(B_6)_1$; *c*) water/oil/$A_6(B_3)_2$; c) water/oil/$A_6(B_2)_3$.

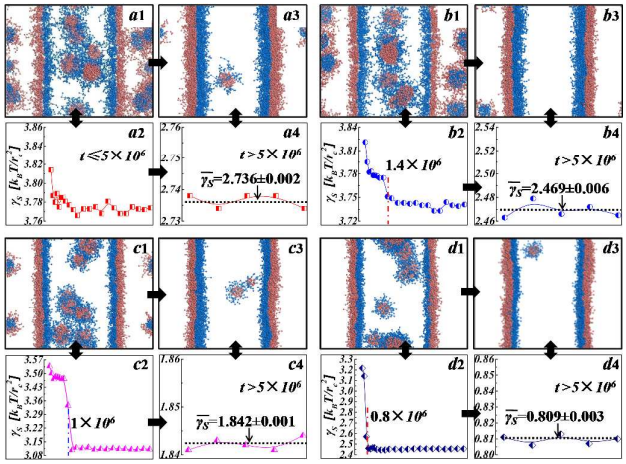

Fig. 4 The evolution of the interface tension γ_S with the simulation time t at φ_{GCP}=0.09. *a*) water/oil/A_6B_6; *b*) water/oil/$A_6(B_6)_1$; *c*) water/oil/$A_6(B_3)_2$; c) water/oil/$A_6(B_2)_3$.

The adsorption of surfactants at the water/oil interface can lower the interfacial tension, which is very important to enhance the crude oil recovery. An essential principle is that we had better reduce the interfacial tension by adding as little surfactants as possible. Therefore, searching the relationship between the interfacial tension (γ_S) and the surfactant concentration (C_S) is very valuable for understanding the mechanism of surfactant efficiency. Figure 5 draws the interfacial tension values as a function of GCP concentrations. As shown in Figure 5, the interfacial tensions show a rapid decrease with the increase of the concentrations for all polymeric surfactants. This is a common phenomenon and in agreement with other simulations and experiments.[3,7,14] Due to the chosen concentrations in this work less than CMC, the familiar plateau of the interfacial tension doesn't appear. In detail, the most reduction of the interfacial tension is about 90% for $\varphi_{A4(B2)2}$=0.09. At the same time, for the fixed concentration, we can find that the efficiency of our used polymeric surfactants on reducing the interfacial tension decreases when the molecular weight increases. For the polymer blend including their block copolymers, Qian et al also obtained the similar results.[21] For the above phenomena, the reason is that the number of surfactant at the interface per area decreases when the molecular weight increases at the fixed concentration, thus the interfacial tension reduction effect decreases.

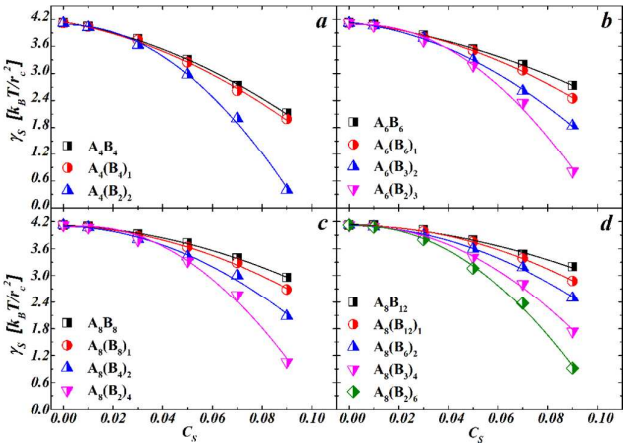

Fig. 5 Interfacial tension γ_S as a function of the concentrations C_S (or φ_{GCP}) of various polymeric surfactants. *a*) water/oil/A4B4 series; *b*) water/oil/A6B6 series; *c*) water/oil/A8B4 series; c) water/oil/A8B12 series.

Interestingly, we can also find that the graft copolymer with more grafts has higher efficacy in reducing the interfacial tension of water/oil interfaces. Taking A6B6 series in Figure 5b as examples, at the higher concentration of φ_{GCP}=0.09, the interfacial tension of ternary systems follows the sequence of $\gamma_{S,A6(B2)3}$=0.809 (3 grafts), $\gamma_{S,A6(B3)2}$=1.842 (2 grafts) and $\gamma_{S,A6(B6)1}$=2.469 (1 grafts). At the medium concentration of φ_{GCP}=0.05, the same sequence can be also found. However, at the lower φ_{GCP}=0.01, the interfacial tension have the ultrafine decrease. We give the simulation results of A4B4, A8B8 and A8B12 series of polymeric surfactants in Figure 5a, 5c and 5d, respectively, the similar conclusions can be also found. The above results testify that the ability of GCPs as surfactants in reducing the interfacial tensions depends on the graft numbers evidently. In fact, several experiments and simulations had also proven the similar viewpoint for polymer blends.[3,5,23] In general, the influence of a surfactant on the interfacial tension is related to the adsorption at the interface. To analyze the adsorption of GCPs at the interface, the density profiles of the oil/water/GCPs ternary system are investigated and the results are given in Figure 6. Figure 6a and 6b draw the density profiles of $A_6(B_2)_3$ and $A_8(B_2)_4$ at the different concentrations of φ_{GCP}=0.01, 0.05 and 0.09, respectively. It is very clear that the adsorption number of surfactants at the interface of oil/water quickly increases with the increase of concentrations for all two GCPs, which confirms the crucial role of the concentration again. In other words, if reducing the interfacial tension of

blends is only one aim, increasing the concentration of surfactants is the best choice. However, the fact is that we hope to add as little surfactants as possible, like the above mentioned. Then, it is important to search the surfactant with the higher efficiency in reducing the interfacial tension at the fixed concentration. To satisfy this requirement, Figure 6c and 6d draw the density curves of A6B6 and A8B8 series of surfactants at the concentrations of φ_{GCP}=0.05 and 0.09, respectively. For the clarity, Figure 6c and 6d only give four $A_6(B_6)_1$, $A_6(B_2)_3$ and $A_8(B_8)_1$, $A_8(B_2)_4$ copolymers at φ_{GCP}= 0.05 as examples, the results clearly show the increase tendency of the adsorption at the interface with the increase of graft numbers.

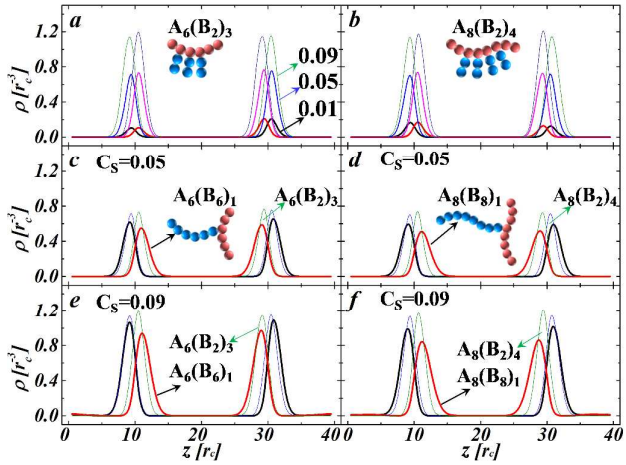

Fig. 6 Density profiles of the typical graft copolymers for the different conditions. It is noted that the two interfaces are generally located at *z*=10 and 30, respectively. Bead A and B are accumulated at the left and right of interfaces, respectively. In detail, distributions of $A_6(B_2)_3$ (a) and $A_8(B_2)_6$ (b) for the concentration of φ_{GCP}=0.01 (most broad lines), 0.05 (middle lines) and 0.09 (thinnest lines); (c) distributions of $A_6(B_6)_1$ (broad lines) and $A_6(B_2)_3$ (thin lines) at φ_{GCP}=0.05; (d) $A_8(B_8)_1$ (broad lines) and $A_8(B_2)_4$ (thin lines) at φ_{GCP}=0.05; (e) $A_6(B_6)_1$ (broad lines) and $A_6(B_2)_3$ (thin lines) at φ_{GCP}=0.09; (f) $A_8(B_8)_1$ (broad lines) and $A_8(B_2)_4$ (thin lines) at φ_{GCP}=0.09.

As for the concentration of φ_{GCP}=0.09 in Figure 6e and 6f, the similar results can also be found. Furthermore, it should be noted that, the high adsorption at the interface can result in the weakly diffusing into the pure phase of two sides. The corresponding density curves show a higher and slimmer shape, as shown in Figure 6c-6f. In fact, the excess adsorption of the graft copolymer surfactants can be well understood from their topological characteristics, as shown in Figure 7. We can suppose that all the polymeric surfactants adopt the completely stretching configuration when they have an ideal close stack at the interface. Then, the familiar linear diblock copolymer A_8B_{12} has the widest distribution (h_{12} and h_8, the subscript number is the bead numbers composing of GCPs) in the direction perpendicular to interface, which corresponds to the smallest interfacial adsorption. Oppositely, the graft copolymer $A_8(B_2)_6$ with 6 grafts has the narrowest distribution (h_2 and h_1) resulting in the highest interfacial density. In the actual interfacial behaviours, it is impossible that all the polymeric surfactants are not completely stretched. However, the order of the distribution extent (h_{12} to h_1) for the different topologies is right.

Except for the interfacial tension, the marked accumulation of surfactants at the interface can also bring the variation of the interfacial thickness (*D*). To understand the influence of graft copolymers on the width of water/oil interface, we calculate

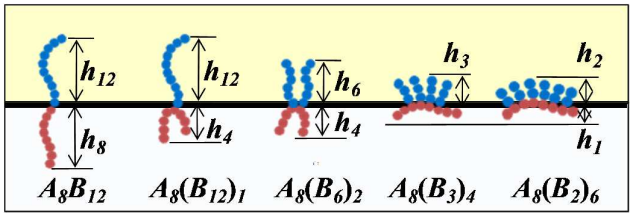

Fig. 7 Schematic of configurations for A8B12 series of graft copolymers at the interface.

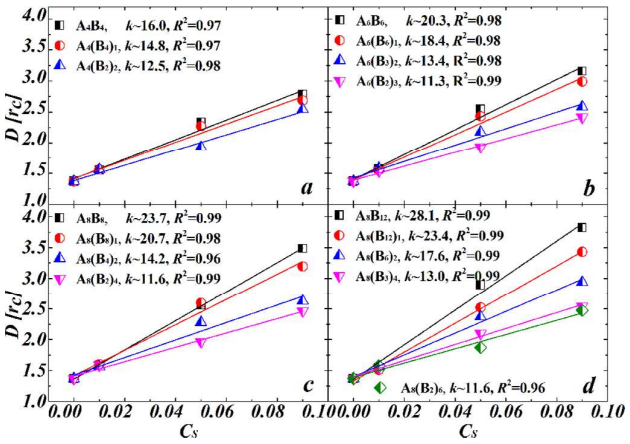

Fig. 8 Interfacial thickness *D* versus the concentrations C_S for various polymeric surfactants. *a*) water/oil/A4B4 series; *b*) water/oil/A6B6 series; *c*) water/oil/A8B4 series; c) water/oil/A8B12 series.

the interfacial thickness by the "90-10" criterion based on the density profiles of oil (or water), which is defined as the distance of the densities of oil from 90% to 10% of their bulk values.[28] Figure 8 gives the fitting relationship, $D=D_0+kC_S$, where *D* is the interfacial thickness of the ternary systems with water, oil and surfactants, C_S (i.e. φ_{GCP}) is the concentration of polymeric surfactants and D_0 is the interfacial thickness of pure binary system (water/oil) without adding polymeric surfactants. Firstly, from Figure 8 we can see a natural phenomenon that the interfacial thickness *D* increases with increasing the concentration of all surfactants. All the fitting correlative coefficients (R^2) are very close to 1, which can powerfully testify that there is a good linear relationship between *D* and C_S. To sum up, the interfacial thickness *D* is constantly broadened with the increase of the concentration C_S no matter how the topological structure of surfactants. It is also in agreement with the analyzed result from the density distributions of surfactants at the interface in Figure 6a and 6b. Secondly, other obvious rule is also found from Figure 8, which is that the slope *k* of all fitting straight lines decreases with the increase of the graft numbers. For example, Figure 8a shows

that the slope *k* of A_4B_4 (no grafts) is equal to 16.0, $A_4(B_4)_1$ with one graft is 14.8 and $A_4(B_2)_2$ with two grafts is 12.5, respectively. This says that the GCPs with more grafts have the lower ability in widening the interfacial thickness than those with fewer grafts. Figure 8b-8d also has the similar rule. Especially, the discrepancy shows more and more obviously with the increase of the concentration. It can be qualitatively explained by the density distributions shown in Figure 6c-6f, which show that the more grafts result in a higher and slimmer distribution of GCPs at two fixed concentrations of φ_{GCP}=0.05 and 0.09. For the interfacial thickness, it is clear that the slimmer distribution plays a negative role, i.e., the decreasing ability of GCPs in increasing the interfacial width. However, for the interfacial tension, the higher distribution plays a positive role, i.e., the increasing ability of GCPs in reducing the interfacial tension. As mentioned above, the similar qualitative understanding of the influence of GCPs on the interfacial tension also had been provided by several significant simulations and theoretical works.[3,23] In this work, through the in-depth analysis of the simulation results, we further find an interesting scaling relationship between the graft number of GCPs and the variation of the interfacial tension before and after adding the GCPS as surfactants. In fact, from Figure 5 we have found that the decreasing degree of the interfacial tension is significant influenced by the graft number of GCPs. The scaling equation is firstly given as

$$\Delta\gamma_S = kC_S^N \tag{5}$$

where the decreasing extent $\Delta\gamma_S=\gamma_S^0-\gamma_S$, γ_S^0 is the interfacial tension of the binary oil/water system and γ_S is the interfacial tension of the ternary oil/water/surfactant system; *k* is a fitting constant related to the total molecular weight; *N* is correlated to the absorption of surfactants at the interface; C_S is the concentration of GCPs (i.e. φ_{GCP}, the volume fraction). The above equation can be rewritten as $log\Delta\gamma_S=logk+N\cdot logC_S$. A plot of $log\Delta\gamma_S$ versus $logC_S$ gives a straight line with a slope of *N*. Figure 9 gives the quantitative results on the plot of $log\Delta\gamma_S$ versus $logC_S$ for the ternary oil/water/GCPs system. In Figure 9a, our simulated *N* values (the slope of the fitting lines) for $A_4(B_4)_1$ (1 graft) and $A_4(B_2)_2$ (2 grafts) surfactants are 1.46 and 1.63, respectively. In brief, the exponent *N* apparently shows an order, $N_{2\ grafts}>N_{1\ graft}$, that are controlled by the graft number. Then, we further check whether other series GCPs of A6B6, A8B8, A8B12 satisfy the similar scaling rule and the results are shown in Figure 9b-9d. Taking $A_8(B_{12})_1$, $A_8(B_6)_2$, $A_8(B_3)_4$ and $A_8(B_2)_6$ GCPs (in Figure 9d) as an example, the *N* values have also the similar order, $N_{6\ grafts}(1.91)>N_{4\ grafts}(1.85)>N_{2\ grafts}(1.69)>N_{1\ graft}(1.61)$, which is close related to the graft number, and the other two series of A6B6 and A8B8 surfactants have also the similar results. The smallest correlation coefficient R^2 in all fitting lines is about 0.95, which ensures the reliability of our statistical analysis. In addition, we can see when the GCP has the same number of grafts, the exponent *N* has very small difference, such as, *N* for 1 graft is in the range of 1.46 to 1.61 and for 2 grafts is about 1.61 to 1.69. Obviously, a very interesting quantitative scaling relation between the topology of GCP surfactants and the interfacial tension is firstly reported by our simulations. Li and co-workers had experimentally established a scaling for the number of latex particles (N_p) and the concentration (*C*) of polymeric surfactants with the different *linear-*, *cyclic-*, and *multiblock-*topologies.[14] The ability of polymeric surfactants reducing the interfacial tension is an important essential factor to influence the number of latex particles. If the interfacial tension can be measured by the experiment, their established relationship ($N_p=kC^{\alpha}$)[14] can also be expressed by the interfacial tension and the topology, as we done. In this way, a more interesting question, whether there is a general scaling relation between the interfacial tension and the topology for all polymeric surfactants, should be considered. It is also the emphasis of our following work.

The increase of surfactant concentrations at the interface is regarded as the crucial factor of influencing the interfacial tension, which is known as the surface excess, Γ_S. Based on the general Gibbs adsorption equation for the dilute systems,

$$\Gamma_S = -\frac{c}{RT}\left(\frac{\partial\gamma}{\partial c}\right)_T \tag{6}$$

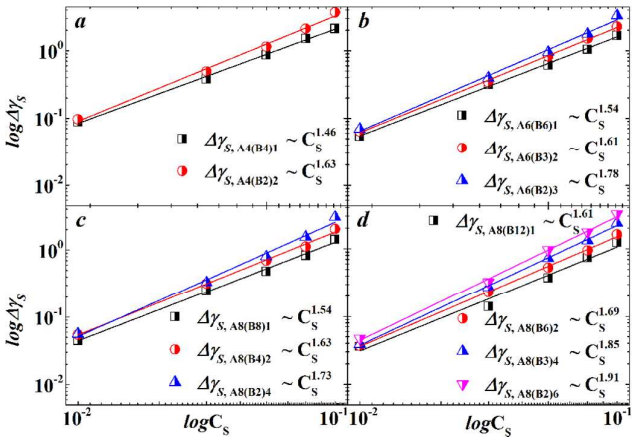

Fig. 9 Surfactant concentrations (C_S) dependence of the variation of interfacial tensions ($\Delta\gamma_S$) for the different series of graft copolymers.

Our new scaling equation $\Delta\gamma_S=\gamma_S^0-\gamma_S=kC_S^N$ in this work can be revised to $\gamma_S-\gamma_S^o=-kC_S^N$, whose first derivative is

$$\frac{d\gamma_S}{dc_S} = -kNC_S^{N-1} \tag{7}$$

Combing the *Eq.*(6) and *Eq.*(7), we can obtain a simple corresponding relation of $NC_S^N \sim \Gamma_S$. It indicates that Γ_S is controlled by the exponent *N*, further by the graft number of GCPs. In other words, the GCP surfactants with more grafts should have the higher surface excess. Additionally, Γ_S can be also calculated from the integral of the density curve of surfactants,[3b]

$$\Gamma_S = \frac{1}{2}\int_0^{Lz}[\rho_{surf}(z) - c_{bulk}]dz \tag{8}$$

That is to say, we can estimate the surface excess from the density profiles of surfactants along the *z* axis normal to the interface, which are given in Figure 6.

Figure 5 has shown that the primacy effect on decreasing the interfacial tension is still the GCP surfactants concentration. Then, combining Gibbs adsorption isotherm, we can deduce a general result that the higher concentration is corresponding to the more surface excess, i.e. $NC_S^N \sim \Gamma_S$. In detail, for the fixed exponent *N*, the variation of density profiles for $A_6(B_2)_3$ and $A_8(B_2)_4$ in Figure 4a and 4b with the increase of concentrations clearly confirms the above deduction. Then, for the fixed concentrations of φ_{GCP}=0.05 and 0.09, Figure 6c to 6f give the density profiles of $A_6(B_6)_1$, $A_6(B_2)_3$ and $A_8(B_8)_1$, $A_8(B_2)_4$ GCPs at the interface, respectively. From the figures, we can clearly see the increase tendency of Γ_S at the interface with the increase of the graft numbers, which is in direct proportion to *N*. This is in good accordance with the analysis results based on Gibbs adsorption isotherm and our simulated scaling relationship. It is different to the general understanding that the polymeric surfactant with the same composition at fixed concentrations should have the same density profile or the surface excess, Γ_S. The topological structures of polymeric surfactants like the concentration also play a significant role.

Conclusions

In summary, a series of DPD simulations are preformed to give insight into the efficacy of well-defined graft copolymers as surfactants in improving the interfacial properties (interfacial tension, interfacial thickness, and so on) of the oil/water system. The general results show that the concentration of GCP surfactants is still the first factor of influencing the interfacial properties. With the increase of the bulk concentrations, the GCPs with more grafts exhibit the lower efficacy in widening the interfacial thickness and the higher efficacy in reducing the interfacial tensions. These results are close related to the adsorption of surfactants at the interface, which is further controlled by the topological structure of surfactants. Importantly, an interesting quantitative scaling relation between the variation of interfacial tensions $\Delta\gamma_S$ and the concentration C_S of surfactants is firstly established, i.e. $\Delta\gamma_S = kC_S^N$. The simulated values of *N* follow the same order of increasing graft numbers, for example, $N_{A8(B8)1} < N_{A8(B4)2} < N_{A8(B2)4}$, which means that the graft copolymers with more grafts as surfactants have the higher ability of reducing the interfacial tension at the same level of concentration. Then, we use Gibbs adsorption isotherm and our established scaling equation to analyses the excess adsorption of surfactants. The results show a good accordance with that from the density profiles of surfactants, i.e. $NC_S^N \sim \Gamma_S$. The more simple method is to directly utilize the topological chain structures to obtain the qualitative similar conclusion. Finally, it should be emphasized that our simulations provide a standard model for experimental applications of graft copolymers as surfactants, especially in reducing the interfacial tensions.

Acknowledgements

All the authors appreciate very much the financial support from Foundation of CAEP (No.2014B0302040, 2014-1-075) and National Nature Sciences Foundation of China (No.11402241).

Notes and references

§ These authors contributed equally to this work.

1 L. S. Romsted, *Surfactant Science and Technology: Retrospects and Prospect*, Taylor & Francis Group: Boca Raton, 2014.
2 J. Traube, *Samml. Chem. Vortr.*, 1899, **4**, 255.
3 (a) L. Rekvig, M. Kranenburg, B. Hafskjold and B. Smit, *Europhys. Lett.*, 2003, **63**, 902; (b) L. Rekvig, M. Kranenburg, J. Vreede, B. Hafskjold and B. Smit, *Langmuir*, 2003, **19**, 8195.
4 B. Creton, C. Nieto-Draghi and N. Pannacc, *Oil Gas Sci. Techn.*, 2012, **6**, 969.
5 Y. W. Xu, C. M. Thurber, T. P. Lodge and M. A. Hillmyer, *Macromolecules*, 2012, **45**, 9604.
6 K. H. Kim and W. H. Jo, *Macromolecules*, 2007, **40**, 3708.
7 P. Venkataraman, J. J. Tang, E. Frenkel, G. L. McPherson, J. B. He, S. Raghavan, V. Kolesnichenko, A. Bose and V. T. John, *ACS Appl. Mater. Interf.*, 2013, **5**, 3572.
8 N. Saleh,T. Sarbu, K. Sirk, G. V. Lowry, K. Matyjaszewski and R. D. Tilton, *Langmuir*, 2005, **21**, 9873.
9 H. Kukula, H. Schlaad and K.Tauer, *Macromolecules*, 2002, **35**, 2538.
10 Y. K. Li, J. Zou, B. P. Das, M. Tsianou and C. Cheng, *Macromolecules*, 2012, **45**, 4623.
11 F. Liu, J. W. Hu, G. J. Liu, S. D. Lin, Y. Y. Tu, C. M. Hou, H. L. Zou, Y. Yang, Y. Wu and Y. M. Mo, *Polym. Chem.*, 2014, **5**, 1381.
12 R. Fenyves, M. Schmutz, I. J. Horner, F. V. Bright and R. Javid, *J. Am. Chem. Soc.*, 2014, **136**, 7762.
13 E. A. Eastwood and M. D. Dadmun, *Macromolecules*, 2002, **35**, 5069.
14 L. W. Li, J. X. Yang, J. F. Zhou, *Macromolecules*, 2013, **46**, 2808.
15 (a) H. Ma, M. X. Luo and L. L. Dai, *Phys. Chem. Chem. Phys.*, 2008, **10**, 2207; (b) S. Liu, R. T. Naga and S. Alberto, *Langmuir*, 2010, **26**, 5462.
16 R. D. Groot and P. B. Warren, *J. Chem. Phys.*, 1997, **107**, 4423.
17 A. Maiti and M. G. Simon, *J. Chem. Phys.*, 2004, **15**, 1594.
18 V. V. Ginzburg, K. Chang, P. K. Jog, A. B. Argenton and L. Rakesh, *J. Phys. Chem. B*, 2011, **115**, 4654.
19 Y. M. Li, Y. Y. Guo, M. T. Bao and X. L. Gao, *J. Colloid Interf. Sci.*, 2011, **361**, 573.
20 (a) H. Fan and A. Striolo, *Phys. Rev. E*, 2012, **86**, 051610; (b) X. C. Luu, J. Yu and A. Striolo, *Langmuir*, 2013, **29**, 7221.
21 H. J. Qian, Z. Y. Lu, L. J. Chen, Z. S. Li and C. C. Sun, J. *Chem. Phys.*, 2005, **122**, 184907.
22 (a) Y. Zhou, X. P. Long and Q. X. Zeng, *J. Appl.Polym. Sci.*, 2012, **125**, 1530; (b) Y. Zhou, X. P. Long and Q. X. Zeng, *Polymer*, 2011, **52**, 6110.
23 (a) Y. Lyatskaya, D. Gersappe, N. A. Gross and A. C. Balazs, *J. Phys. Chem.*, 1996, **100**, 1449; (b) Y. Lyatskaya, S. H. Jacobson and A. C. Balazs, *Macromolecules*, 1996, **29**, 1059; (c) Y. Lyatskaya, D. Gersappe, and A. C. Balazs, *Macromolecules*, 1996, **28**, 6278; (d) R. Israels, D. P. Foster and A. C. Balazs, *Macromolecules*, 1995, **28**, 218; (e) D. Gersappe, P. K. Harm, D. Irvine and A. C. Balazs, *Macromolecules*, 1994, **27**, 720.
24 P. J. Hoogerbrugand J. M. V. A. Koelman, *Europhys. Lett.*, 1992, **19**, 155.
25 P. Español and P. B. Warren, *Europhys. Lett.*, 1995, **30**, 191.

26 Z. X. Chen, X. L. Cheng, H. S. Cui, P. Cheng, H. Y. Wang, *Colloids and Surfaces A: Physicochem. Eng. Aspects*, 2007, **30**, 1437.
27 J. Alejandre, J. L. Rivera, M. A. Mora and D. V. Garza, *J. Phys. Chem. B*, 2000, **104**, 1332.
28 M. X. Luo and L. L. Dai, *J. Phys.: Condens. Matter*, 2007, **19**, 375109.